Journal of Nuclear Materials 384 (2009) 231–235

Contents lists available at ScienceDirect

Journal of Nuclear Materials

journal homepage: www.elsevier.com/locate/jnucmat

Calorimetric measurements on $(U,Th)O_2$ solid solutions

R. Kandan, R. Babu, P. Manikandan, R. Venkata Krishnan, K. Nagarajan *

Fuel Chemistry Division, Chemistry Group, Indira Gandhi Centre for Atomic Research, Department of Atomic Energy, Kalpakkam, 603 102, India

ARTICLE INFO

Article history:
Received 17 April 2008
Accepted 19 November 2008

ABSTRACT

Enthalpy increments of urania – thoria solid solutions, $(U_{0.10}Th_{0.90})O_2$, $(U_{0.50}Th_{0.50})O_2$ and $(U_{0.90}Th_{0.10})O_2$ were measured by drop calorimetry in the temperature range 479 – 1805 K. Heat capacity, entropy and Gibbs energy function were computed. The heat capacity measurements were carried out also with differential scanning calorimetry in the temperature range 298 – 800 K. The heat capacity values of $(U_{0.10}Th_{0.90})O_2$, $(U_{0.50}Th_{0.50})O_2$ and $(U_{0.90}Th_{0.10})O_2$ at 298 K are 59.62, 61.02, 63.56 J K^{-1} mol^{-1}, respectively. The results were compared with the data available in the literature. From the study, the heat capacity of $(U,Th)O_2$ solid solutions was shown to obey the Neumann – Kopp's rule.

1. Introduction

Urania – thoria solid solutions are being considered as fuels for thermal breeder reactors such as the Advanced Heavy Water Reactor (AHWR) being planned in India and high temperature gas cooled reactors [1,2]. Under these situations, the thermodynamic properties of these mixed oxides are necessary for understanding the fuel behavior during irradiation and for predicting the performance of the fuel under accidental conditions. The thermodynamic properties of ThO_2 and $(U,Th)O_2$ were reviewed by Fink [3,4] and Bakker et al. [5]. Those of UO_2 were reviewed also by Fink [3,4]. Springer et al. [6] measured the enthalpy increments of $(U_{0.20}Th_{0.80})O_2$ and $(U_{0.10}Th_{0.90})O_2$ in the temperature range 273 – 2271 K using Bunsen ice calorimeter. Fischer et al. [7] measured the enthalpy increments of $(U_{0.08}Th_{0.92})O_2$, $(U_{0.15}Th_{0.85})O_2$ and $(U_{0.30}Th_{0.70})O_2$, in the temperature range 2300 – 3400 K, using an induction heated drop calorimeter. The enthalpy increments of $(U_{0.0196}Th_{0.9804})O_2$, $(U_{0.0390}Th_{0.9610})O_2$, $(U_{0.0590}Th_{0.9410})O_2$ and $(U_{0.0980}Th_{0.9020})O_2$ were measured by Agarwal et al. [8] in the temperature range 375 – 991 K using a Calvet calorimeter. The enthalpy increments of $(U_{0.10}Th_{0.90})O_2$, $(U_{0.50}Th_{0.50})O_2$ and $(U_{0.90}Th_{0.10})O_2$ were measured by Anthonysamy et al. [9] in the temperature range 473 – 973 K using an in-house built conventional isoperibol type drop calorimeter. Most of the enthalpy increment and heat capacity data for $(U,Th)O_2$ available in the literature are for thoria-rich ($\leqslant$20 mol% of urania) solid solutions, and the data available for wider composition range are those in the limited temperature ranges [6–9]. In this study, calorimetric measurements have been carried out covering wider temperature and composition ranges. The enthalpy increments of $(U_{0.10}Th_{0.90})O_2$, $(U_{0.50}Th_{0.50})O_2$ and $(U_{0.90}Th_{0.10})O_2$ were measured in the present study using a high temperature drop calorimeter in the temperature range 479 – 1805 K. The heat capacity measurements were also made using a differential scanning calorimeter (DSC), in the temperature range 298 – 800 K. The results of these measurements are compared and discussed.

2. Experimental

2.1. Preparation and characterization of $(U,Th)O_2$

Urania – thoria solid solutions were prepared by co-precipitation of ammonium diuranate and thorium hydroxide from a mixture of uranyl nitrate and thorium nitrate solutions by the addition of aqueous ammonia followed by drying and calcination at 1073 K in air for 5 h. The calcined powders were then compacted at 500 MPa to form pellets of 10 mm diameter and 2 – 3 mm height without using any binder or lubricant and the pellets were sintered at 1873 K for 6 h in flowing Ar – 8 vol.% H_2 gas mixture. The O/M ratios of the pellets were fixed at 2.00 by equilibration at 1073 K with H_2 – H_2O gas mixture having an oxygen potential of −450 kJ mol^{-1}. The phase analysis of the samples was made by the use of the X-ray diffraction method. The X-ray diffraction measurements were carried out using a wide angle goniometer of X'PERT MPD system supplied by M/s. Philips, The Netherlands. The X-ray diffraction patterns of the pellets were obtained using Cu-K_α radiation monochromatized with curved graphite monochromator. The XRD patterns of the solid solutions did not show any peaks of each of uranium and thorium dioxides. The diffraction patterns of the solid solutions are given in Fig. 1. Lattice parameters were calculated using the high angle reflections. Selected diffraction angles were determined accurately by scanning slowly across the peaks. The approximate lattice parameters calculated

---

* Corresponding author.
E-mail address: knag@igcar.gov.in (K. Nagarajan).

0022-3115/$ - see front matter © 2008 Elsevier B.V. All rights reserved.
doi:10.1016/j.jnucmat.2008.11.012

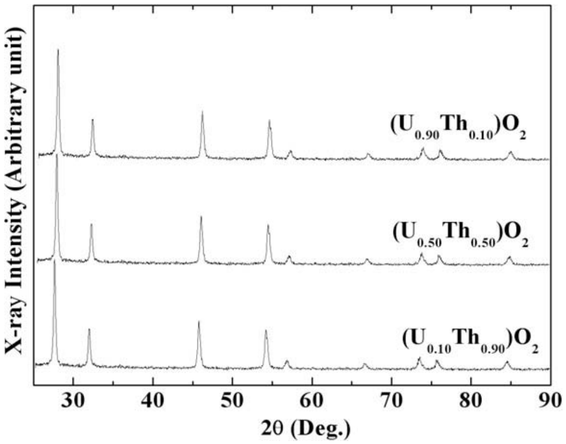

Fig. 1. Room temperature XRD patterns of $(U,Th)O_2$ solid solutions.

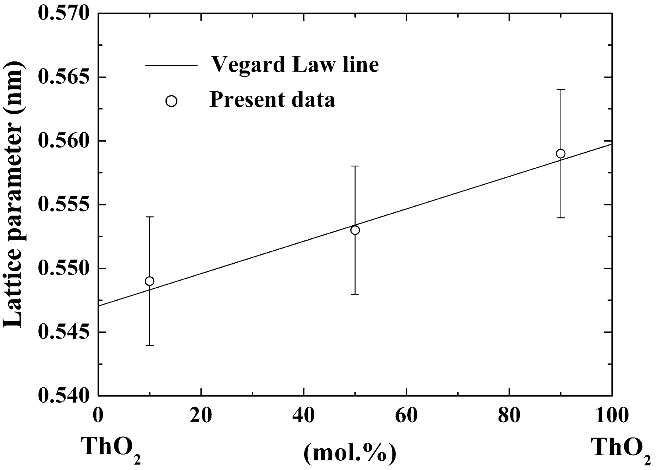

Fig. 2. Lattice parameters of $(U,Th)O_2$ solid solutions as a function of Th concentration.

from the Miller indices and reflection angles were refined by the method of least squares using the computer programme AIDS 83. The XRD data were obtained in the 2θ range varying from 20 to 90°. An effective high angle corrected lattice parameter for each composition was determined using Nelson – Riley interpolation scheme [10]. The estimated error in the lattice parameters is within ±0.005 nm. In Fig. 2, the lattice parameters of the solid solutions are plotted and compared with the Vegard's law line which represents a linear variation between the recommended lattice parameters of ThO_2 and UO_2. The very good agreement between the Vegard's law line and the lattice parameters of the solid solutions observed could be considered as an indication of an ideal solid solution. The lattice parameters, densities, theoretical and sintered densities of the uranium – thorium mixed oxide pellets used in this study are given in Table 1.

Table 1
Physical properties of $(U,Th)O_2$ solid solutions.

Sample	Lattice parameter (nm)	Theoretical density (g/cm^3)	Sintered density	
			Measured (g/cm^3)	Percent of theoretical density (%)
$(U_{0.10}Th_{0.90})\ O_2$	0.559	10.084	9.957	98.73
$(U_{0.50}Th_{0.50})\ O_2$	0.553	10.494	9.867	94.02
$(U_{0.90}Th_{0.10})\ O_2$	0.549	10.732	10.136	94.46

2.2. Enthalpy increment measurements by drop calorimetry

A 'multi-detector' high temperature calorimeter (MHTC-96) of M/s. SETARAM, France was employed for enthalpy increment measurements on $(U,Th)O_2$ solid solutions. It functions as an isoperibol type calorimeter, which measures heat flow between a reference and a sample crucible using a calorimetric detector. The calorimetric detector is composed of 36 Pt – 6%Rh/Pt – 30%Rh thermocouples connected in series in which a sample and an empty reference crucible are positioned one above the other.

In a typical experiment, five pairs of the samples of α-alumina reference (SRM 720) and ~5 mmΦ $(U,Th)O_2$ pellets, each weighing about 150 – 200 mg, were placed in the individual slots of the specimen holder kept at room temperature. The $(U,Th)O_2$ samples and the Al_2O_3 references were loaded in such a way that each sample was sandwiched between two Al_2O_3 references. The furnace was then gradually heated to the desired experimental temperature under Ar cover gas. Once the temperature of the furnace reached the preset value, the specimens were dropped alternatively from the specimen holder, maintained at the ambient temperature, into the sample crucible of the experimental temperature. From the resultant heat flow signals corresponding to the alumina reference and the $(U,Th)O_2$ sample, the enthalpy increments of the $(U,Th)O_2$ samples were determined, using the critically accessed enthalpy increment values of the reference [11]. The mean of the five heat flow values for the standard and that for the sample were used to compute the enthalpy increment at that temperature, T. The experiment was repeated 4 or 5 times at the same temperature T, and the mean value of the enthalpy increments from these runs at temperature, T are taken for fitting.

2.3. Heat capacity measurements by DSC

A heat flux type differential scanning calorimeter, model number DSC 821e/700 of M/s. Mettler Toledo GmbH, Switzerland, was used. Heat flow rate calibration was performed, prior to each heat capacity measurement, with a disc of sapphire supplied by M/s. Mettler Toledo GmbH, Switzerland, using the heat capacity data of sapphire from NIST, USA [11]. The description of the calorimeter, its heat flow and temperature calibrations and the procedure for heat capacity measurements have been described in detail elsewhere [12].

3. Results

3.1. Enthalpy increments

The accuracy of the enthalpy increment measurements was determined to be ±2.5% from the measurements on ThO_2. The temperature of the sample was measured with an accuracy of ±0.1 K. The enthalpy increments of $(U_{0.10}Th_{0.90})O_2$, $(U_{0.50}Th_{0.50})O_2$ and $(U_{0.90}Th_{0.10})O_2$ were measured in the temperature ranges of 486 – 1775, 486 – 1758 and 479 – 1805 K, respectively. The measured enthalpy values were fitted to 4-term polynomial functions of the below form by using the least-squares method:

$$(H_T - H_{298})/\mathrm{kJ\ mol^{-1}} = AT + BT^2 + C/T + D \tag{1}$$

The constraints used for the fitting were: (a) $H_T - H_{298} = 0$ at 298 K and (b) the derivative of the function at 298 K to be equal to C_P at 298 K (59.62, 61.02, 63.56 J K^{-1} mol^{-1}, respectively) of the solid solutions determined in this study by DSC measurements. The standard errors of the fits were 0.2, 0.98 and 0.9%, and the standard deviations for the fits were 146, 667 and 617 J mol^{-1}, respectively. The S_{298} values needed for the computation of the entropy and Gibbs energy functions were also estimated from

Table 2

$C_{P,298}$ and S_{298}values of (U,Th)O_2 solid solutions used for computations.

Solid solution	$C_{P,\ 298}$ (J K^{-1} mol^{-1}) (DSC)	S_{298} (J K^{-1} mol^{-1}) (Neumann–Kopp's rule)
$(U_{0.10}Th_{0.90})\ O_2$	59.62	69.08
$(U_{0.50}Th_{0.50})\ O_2$	61.02	76.86
$(U_{0.90}Th_{0.10})\ O_2$	63.56	78.52

Table 3

Constants for the fit equation of enthalpy increments (drop calorimetry) $H_T{-}H_{298}$/kJ mol^{-1} = $AT + BT^2 + C/T + D$.

Solid solution	A	$B \times 10^3$	$C \times 10^{-5}$	D	T (K)
$(U_{0.10}Th_{0.90})\ O_2$	77.554	1.548	16.763	−28883	298–1800
$(U_{0.50}Th_{0.50})\ O_2$	75.946	2.974	14.844	−27886	298–1800
$(U_{0.90}Th_{0.10})\ O_2$	74.927	4.548	12.516	−26942	298–1800

Table 4

Thermodynamic functions of $(U_{0.10}Th_{0.90})O_2$.

T	$H_T{-}H_{298}$		T	$H_T{-}H_{298}$	C_P	S_T	$-(G_T{-}H_{298})/T$
	Measured	Fitted					
(K)	(kJ mol^{-1})	(kJ mol^{-1})	(K)	(kJ mol^{-1})	(J K^{-1} mol^{-1})		
486	12.597	12.623	298	0	59.62	69.08	69.08
588	20.045	20.105	300	0.111	59.86	69.45	69.08
689	27.611	27.720	400	6.577	68.32	87.99	71.56
787	35.286	35.241	500	13.634	72.40	103.73	76.46
890	42.970	43.250	600	21.001	74.76	117.15	82.15
989	51.140	51.028	700	28.559	76.30	128.80	88.0
1091	59.188	59.108	800	36.247	77.41	139.07	93.76
1192	67.060	67.168	900	44.033	78.27	148.24	99.31
1291	75.186	75.119	1000	51.896	78.98	156.52	104.62
1391	83.377	83.196	1100	59.824	79.58	164.08	109.69
1491	91.493	91.317	1200	67.809	80.11	171.02	114.51
1591	99.287	99.479	1300	75.844	80.59	177.45	119.11
1689	107.480	107.516	1400	83.925	81.03	183.44	123.50
1775	114.576	114.599	1500	92.050	81.45	189.05	127.68
			1600	100.215	81.85	194.32	131.68
			1700	108.420	82.24	199.29	135.51
			1800	116.663	82.61	204.00	139.19

the literature data for the S^0_{298} values of UO_2 [4] and ThO_2 [5] by using Neumann – Kopp's rule and adding ideal mixing entropy. The values of $C_{P,298}$ and S_{298} used for computation of thermodynamic functions are given in Table 2. The values of the constants in the above fit equation obtained for $(U_{0.10}Th_{0.90})O_2$, $(U_{0.50}Th_{0.50})O_2$ and $(U_{0.90}Th_{0.10})O_2$ are given in Table 3. The enthalpy, heat capacity, entropy and Gibbs free energy functions of $(U_{0.10}Th_{0.90})O_2$, $(U_{0.50}Th_{0.50})O_2$ and $(U_{0.90}Th_{0.10})O_2$ computed are given in Tables 4–6, respectively along with their measured enthalpy increment values.

3.2. Heat capacity

The accuracy of the heat capacity measurements by DSC was determined to be ±1% from the measurements on ThO_2. The temperature of the sample was measured with an accuracy of ±0.5 K. The heat capacity of each solid solution reported here is the mean of nine or 10 measurements. The relative standard deviation is 2 – 3%. The measured heat capacity values of $(U_{0.10}Th_{0.90})O_2$, $(U_{0.50}Th_{0.50})O_2$ and $(U_{0.90}Th_{0.10})O_2$ were least-square fitted to obtain the following polynomials of temperature in the range 298 – 800 K

$$C_P(U_{0.10}Th_{0.90})O_2/(\mathrm{J\ K^{-1}\ mol^{-1}}) = 71.63 + 10.65 \times 10^{-3}T - 13.56 \times 10^5/T^2 \quad (2)$$

$$C_P(U_{0.50}Th_{0.50})O_2/(\mathrm{J\ K^{-1}\ mol^{-1}}) = 73.47 + 11.48 \times 10^{-3}T - 14.23 \times 10^5/T^2 \quad (3)$$

$$C_P(U_{0.90}Th_{0.10})O_2/(\mathrm{J\ K^{-1}\ mol^{-1}}) = 73.63 + 14.79 \times 10^{-3}T - 12.89 \times 10^5/T^2 \quad (4)$$

The standard errors of the fits were 0.993, 0.998 and 0.995 J K^{-1} mol^{-1}, respectively.

4. Discussion

The measured enthalpy increments of $(U_{0.10}Th_{0.90})O_2$, $(U_{0.50}Th_{0.50})O_2$ and $(U_{0.90}Th_{0.10})O_2$ along with the fit values are shown in Fig. 3. The enthalpy increment values of $(U_{0.10}Th_{0.90})O_2$, $(U_{0.50}Th_{0.50})O_2$ and $(U_{0.90}Th_{0.10})O_2$ computed by the Neumann – Kopp's rule using the heat capacity data of UO_2 [4] and ThO_2 [5] are also shown in Fig. 3. As can be seen from Fig. 3, as well as from Tables 4–6, the enthalpy increment values for the three compositions decrease with increase in ThO_2 content. However, the difference between the enthalpy increment data of solid solutions $(U_{0.50}Th_{0.50})O_2$ and $(U_{0.10}Th_{0.90})O_2$ are within 2.5%, the error in our measurements. The present enthalpy increment data are in very good agreement with those computed by using the Neumann – Kopp's rule within ±1 – 2% for the solid solutions of three compositions. In Fig. 4, the present enthalpy increment values of $(U_{0.10}Th_{0.90})O_2$ are compared with literature data [6–9]. The $(H_T{-}H_{273})$ values of Springer et al. [6] were corrected to $(H_T{-}H_{298})$ by subtracting $(H_{298}{-}H_{273})$ using their polynomial and compared with the present data. The present enthalpy increments of $(U_{0.10}Th_{0.90})O_2$ are 1.5% higher than those of Springer et al. [6] throughout the whole temperature range, 1% higher than those of Anthonysamy et al. [9], and 2% higher than those of Agarwal et al. [8]. In Fig. 5, the heat capacities for all three solid solutions obtained from drop calorimetric enthalpy increment values are compared. The heat capacity data computed from drop calorimetric values are in very good agreement with those obtained by the Neumann – Kopp's rule. However, in the case of $(U_{0.90}Th_{0.10})O_2$ some of the fit heat capacity data are slightly higher than those of UO_2. But the deviations are within the experimental uncertainties. The heat capacity increases with increase in UO_2 content. The increasing trend of the anomalous increase in heat capacity of UO_2 above 1200 K could also be observed with increasing UO_2 content in Fig. 5. The measured heat capacity values of $(U_{0.10}Th_{0.90})O_2$, $(U_{0.50}Th_{0.50})O_2$ and $(U_{0.90}Th_{0.10})O_2$ by DSC along with the fit values are shown in Fig. 6. The heat capacity data of $(U_{0.10}Th_{0.90})O_2$, $(U_{0.50}Th_{0.50})O_2$ and $(U_{0.90}Th_{0.10})O_2$ computed by the Neumann – Kopp's rule using the heat capacity data of UO_2 [4] and ThO_2 [5] are also shown in Fig. 6. As can be seen from the figure, the heat capacity values by DSC measurements are in agreement with the values computed by using the Neumann – Kopp's rule within ±2% for all the three solid solutions. In Fig. 7, the heat capacity of (U,Th)O_2 solid solutions calculated from drop calorimetric measurements are compared with the values measured by DSC. The heat capacity values computed from the drop calorimetric measurements are in agreement with the values measured by DSC within 1.3% for $(U_{0.10}Th_{0.90})O_2$ and 2 – 4% for the other two, the DSC values always being higher.

5. Conclusion

Enthalpy increments of urania – thoria solid solutions, $(U_{0.10}Th_{0.90})O_2$, $(U_{0.50}Th_{0.50})O_2$ and $(U_{0.90}Th_{0.10})O_2$ were measured by employing the method of inverse drop calorimetry in the temperature range 479 – 1805 K using multi-detector high temperature calorimeter. Heat capacity measurements were also carried out on these solid solutions in the temperature range 298

Table 5
Thermodynamic functions of $(U_{0.50}Th_{0.50})O_2$.

T	H_T–H_{298}		T	H_T–H_{298}	C_P	S_T	–$(G_T$–$H_{298})/T$
	Measured	Fitted					
(K)	(kJ mol^{-1})	(kJ mol^{-1})	(K)	(kJ mol^{-1})	(J K^{-1} mol^{-1})		
486	12.768	12.780	298	0	61.02	76.86	76.86
588	20.484	20.322	300	0.113	61.24	77.24	76.86
689	28.221	28.006	400	6.679	69.05	96.08	79.38
790	36.649	35.846	500	13.799	72.98	111.95	84.35
890	43.270	43.729	600	21.226	75.39	125.48	90.11
991	52.627	51.794	700	28.853	77.08	137.24	96.02
1091	58.678	59.870	800	36.629	78.38	147.62	101.83
1185	68.195	67.537	900	44.523	79.47	156.91	107.44
1286	76.011	75.852	1000	52.517	80.41	165.34	112.82
1387	84.526	84.241	1100	60.601	81.26	173.04	117.95
1487	91.286	92.618	1200	68.767	82.05	180.15	122.84
1587	100.459	101.064	1300	77.010	82.80	186.74	127.50
1687	110.122	109.576	1400	85.326	83.51	192.91	131.96
1758	116.174	115.660	1500	93.712	84.21	198.69	136.22
			1600	102.167	84.88	204.15	140.29
			1700	110.688	85.54	209.31	144.20
			1800	119.275	86.19	214.22	147.96

Table 6
Thermodynamic functions of $(U_{0.90}Th_{0.10})O_2$.

T	H_T–H_{298}		T	H_T–H_{298}	C_P	S_T	–$(G_T$–$H_{298})/T$
	Measured	Fitted					
(K)	(kJ mol^{-1})	(kJ mol^{-1})	(K)	(kJ mol^{-1})	(J K^{-1} mol^{-1})		
479	12.900	12.605	298	0	63.56	78.52	78.52
583	20.630	20.434	300	0.118	63.75	78.92	78.52
684	28.765	28.266	400	6.886	70.74	98.34	81.13
785	35.704	36.273	500	14.162	74.47	114.56	86.24
885	43.260	44.345	600	21.738	76.91	128.37	92.14
986	53.004	52.628	700	29.524	78.74	140.37	98.19
1086	61.366	60.946	800	37.476	80.25	150.98	104.14
1187	69.370	69.460	900	45.568	81.57	160.51	109.88
1287	77.820	77.996	1000	53.785	82.77	169.17	115.38
1387	86.384	86.635	1100	62.119	83.90	177.11	120.64
1488	95.380	95.462	1200	70.563	84.97	184.46	125.65
1588	105.170	104.300	1300	79.113	86.01	191.30	130.44
1689	113.960	113.326	1400	87.765	87.02	197.71	135.02
1805	122.912	123.814	1500	96.517	88.02	203.75	139.40
			1600	105.368	88.99	209.46	143.61
			1700	114.315	89.96	214.88	147.64
			1800	123.359	90.91	220.05	151.52

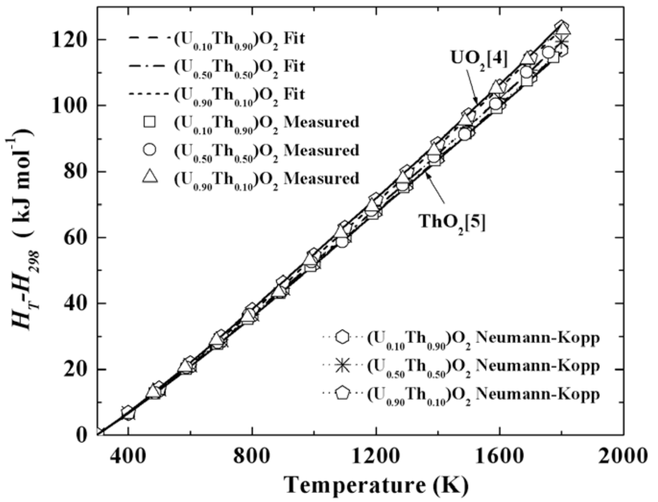

Fig. 3. Enthalpy increments of $(U,Th)O_2$ solid solutions by drop calorimetry.

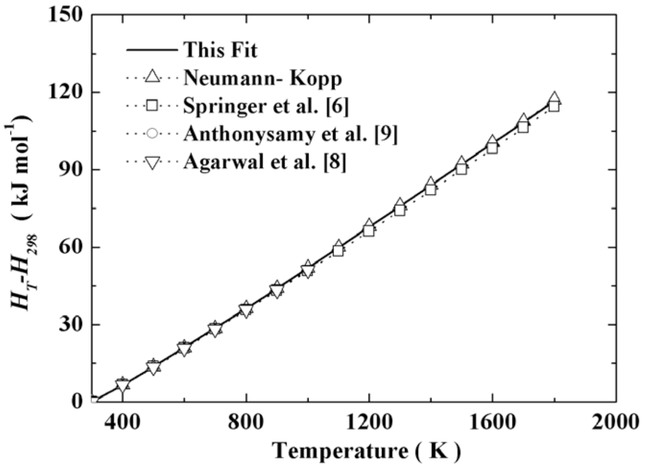

Fig. 4. Comparison of the enthalpy increments of $(U_{0.10}Th_{0.90})O_2$ with literature data.

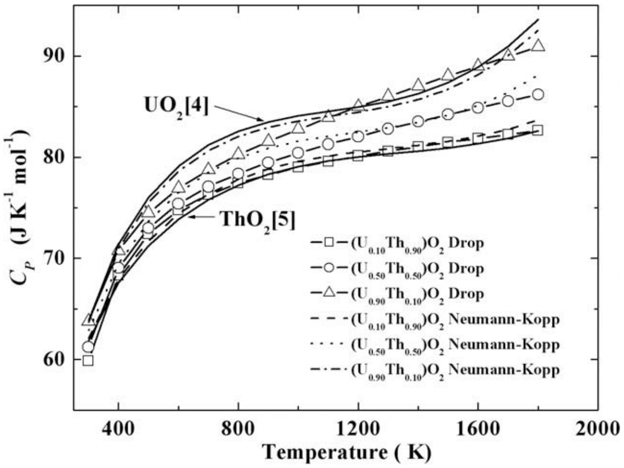

Fig. 5. Comparison of the heat capacity data of (U,Th)O_2 computed from enthalpy increments with values calculated by the Neumann–Kopp's rule.

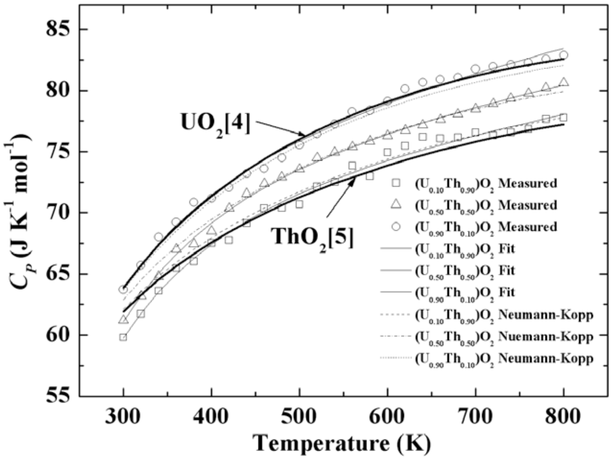

Fig. 6. Heat capacity of (U,Th)O_2 solid solutions by DSC.

– 800 K by differential scanning calorimetry. Other thermodynamic functions, namely, heat capacity, entropy and Gibbs energy functions were computed in the temperature range 298 – 1800 K. The results indicate that the enthalpies of (U,Th)O_2 solid solutions in the temperature range 298 – 1800 K obey the Neumann – Kopp's rule.

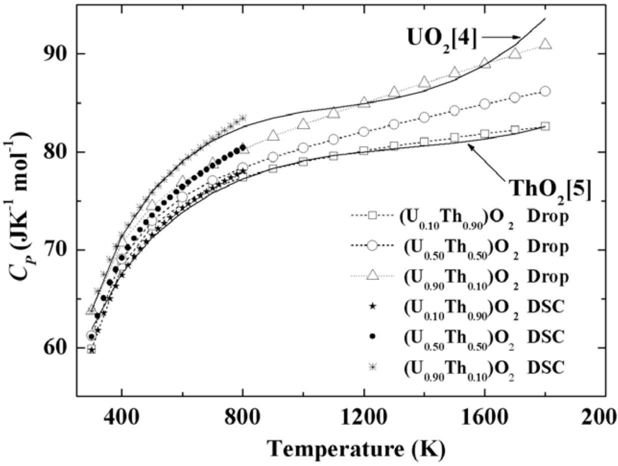

Fig. 7. Comparison of the heat capacities of (U,Th)O_2 solid solutions computed from drop calorimetry with those measured by DSC.

References

[1] C. Ganguly, IAEA-TECDOC 352 (1985) 107.
[2] C. Ganguly, in: P. Vincenzini (Ed.), High Tech. Ceramics, Elsevier, Amsterdam, 1987, p. 2887.
[3] J.K. Fink, J. Thermophys. 3 (1982) 165.
[4] J.K. Fink, J. Nucl. Mater. 279 (2000) 1.
[5] K. Bakker, E.H.P. Cordfunke, R.J.M. Konings, R.P.C. Scharm, J. Nucl. Mater. 250 (1997) 1.
[6] J.R. Springer, E.A. Eldridgh, N.U. Goodyear, T.R. Wright, J.F. Lagedrox, Battelle Memorial Institute Report, BMI-X-10210, October 1967.
[7] D.F. Fischer, J.K. Fink, L. Leibowitz, J. Nucl. Mater. 118 (1983) 342.
[8] R. Agarwal, R. Prasad, V. Venugopal, J. Nucl. Mater. 322 (2003) 98.
[9] S. Anthonysamy, Jose Joseph, P.R. Vasudeva Rao, J. Nucl. Mater. 299 (2000) 112.
[10] B.D. Cullity, Elements of X-ray Diffraction, Second ed., Addison-Wesely Co., Reading, MA, 1978 (Chapter 11).
[11] Synthetic Sapphire Al_2O_3, Certificate of Standard Reference Materials, SRM 720, 1982.National Bureau of Standards, U.S. Department of Commerce, Washington, DC 20234,USA.
[12] R. Venkata Krishnan, K. Nagarajan, Thermochim. Acta 440 (2006) 141.